論文 / 著書情報
Article / Book Information

Title	Locally amplified tsunami in Iida Bay due to the 2024 Noto Peninsula Earthquake
Authors	Hiroshi Takagi, Nabiel Luthfi Siddiq, Feldy Tanako, Daryl Paul Balita De La Rosa
Citation	Ocean Engineering, Vol. 307, ,
Pub. date	2024, 5
DOI	https://dx.doi.org/10.1016/j.oceaneng.2024.118180

Ocean Engineering 307 (2024) 118180

Contents lists available at ScienceDirect

Ocean Engineering

journal homepage: www.elsevier.com/locate/oceaneng

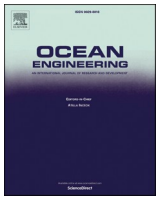

Research paper

Locally amplified tsunami in Iida Bay due to the 2024 Noto Peninsula Earthquake

Hiroshi Takagi *, Nabiel Luthfi Siddiq, Feldy Tanako, Daryl Paul Balita De La Rosa

School of Environment and Society, Tokyo Institute of Technology, 2-12-1 Ookayama, Meguro, Tokyo, 152-8550, Japan

ARTICLE INFO

Keywords:
2024 Noto Peninsula earthquake
Iida bay
Tsunami amplification
Breakwater damage
Field survey
Numerical simulation

ABSTRACT

The 2024 Noto Peninsula Earthquake in Japan generated tsunamis of over 3 m high in Iida Bay, causing extensive damage to ports and residential areas. The tsunamis observed in Iida Bay were remarkably higher than those at other coasts, and it can be inferred that some mechanisms may have amplified the tsunami. This study aimed to elucidate why tsunami damage was concentrated in Iida Bay. A numerical simulation showed that the tsunami energy propagating from the earthquake source fault toward Toyama Bay converged on the edge between the shallow sea (Iida Spur) and the deep sea (Toyama Trough). The concentrated tsunami energy then propagated into Iida Bay, triggering multiple secondary short-period tsunamis. According to video monitoring overlooking Iida Bay, a bore-like tsunami propagating along the coastline intersected with a tsunami directly reaching Iida Port, resulting in an over 10-m high splash when it hit the breakwater. Wavelet analysis of the computational output showed that the primary tsunami energy had an oscillation period of 5–10 min, whereas that of the secondary tsunami energy was less than 2 min. The superposition of these multiple waves most likely caused the locally amplified tsunami in Iida Bay.

1. Introduction

The 2024 Noto Peninsula Earthquake (Mw 7.5) on New Year's Day 2024 caused strong shaking, tsunami, severe liquefaction, landside, and fire on the Noto Peninsula, resulting in extensive damage to numerous buildings and infrastructure. In Ishikawa Prefecture, the hardest-hit area, at least 241 people died, and 75,187 houses were damaged (as of February 21, 2024, NHK, 2024). The northern coast of the Noto Peninsula was uplifted by up to 4 m (Geospatial Information Authority of Japan, 2024a; Geological Survey of Japan, 2024a), making the launch of vessels from certain ports, such as Kaiso Fishing Port and Wajima Port, impossible. In the Ishikawa, Toyama, and Niigata prefectures, 1.3–5.8 m high tsunamis were confirmed (Japan Meteorological Agency, 2024). Tsunamis were observed in these most affected prefectures and over a wide area on the Japan Sea side. For example, according to tide observation data, tsunami waves of 60 cm was observed in Setana Town, Hokkaido Prefecture, 600 km from the epicenter, 135 min after the earthquake, and 20-cm waves were observed in Oki Island Town, Shimane Prefecture, 370 km from the epicenter, 100 min after the earthquake.

The Noto Peninsula has been frequently hit by tsunamis caused by earthquakes that occurred at relatively remote locations along the eastern margin of the Sea of Japan. For example, in 1883, a tsunami generated off the coast of Yamagata struck Wajima on the Noto Peninsula, killing 47 people (Hatori, 1990). Those past tsunamis generated in the Japan Sea amplified around the Noto Peninsula due to refraction and wave shoaling (Hatori, 1990). In the past four major tsunamis that hit the Noto Peninsula (1833 Yamagata-oki, 1741 Oshima-Oshima, 1964 Niigata-oki, and 1983 Central Japan Sea Earthquake), high tsunamis hit the northern coast of the Noto Peninsula, whereas the estimated tsunamis in the southern side of the peninsula, including Toyama Bay, were lower (Yuhi and Abe, 2013). The 2024 Noto Peninsula Earthquake caused significant tsunami damage particularly on the Toyama Bay side of the Noto Peninsula. The characteristics of this event was different from those previous tsunamis.

Although the disaster area was challenging to access, researchers from universities across Japan, governmental agencies such as the Japan Meteorological Agency and the Geospatial Information Authority of Japan, and academic societies such as the Japan Society of Civil Engineers and the Architectural Institute of Japan actively conducted post-disaster surveys to identify traces of the tsunami immediately after the earthquake.

* Corresponding author.
E-mail address: takagi.h.ae@m.titech.ac.jp (H. Takagi).

https://doi.org/10.1016/j.oceaneng.2024.118180
Received 8 April 2024; Received in revised form 6 May 2024; Accepted 12 May 2024
Available online 19 May 2024

The tsunamis that hit Iida Bay, which is located near the epicenter of the earthquake, were remarkably higher than those that hit the other coasts of the Noto Peninsula. For example, places experiencing inundation heights exceeding 3 m were primarily concentrated in Iida Bay. Additionally, places with the runup heights exceeding 3 m, which typically exceed inundation heights, were confirmed in Joetsu City and Sado City in Niigata Prefecture (Japan Meteorological Agency, 2024). The area surrounding Ukai Fishing Port in Iida Bay was the most widely inundated by the tsunami, and an aerial photo image and field surveys revealed that the area was inundated up to approximately 500 m inland from the coast (Geological Survey of Japan, 2024b). Additionally, some sections of the breakwater at Iida Port collapsed (Nikkei XTECH, 2024), suggesting that the tsunami was concentrated and amplified through unique mechanisms.

In this study, tsunami behavior and characteristics in Iida Bay were investigated in detail based on a field survey, numerical analysis, and video recordings from a monitoring camera to clarify whether the tsunami impact in this semi-closed bay was magnified via a unique mechanism.

2. Material and methods

Parameters for the model of the earthquake source fault that generated the tsunamis included the location and shape of the fault model (length, width, strike, and dip), scale (fault area and seismic moment), slip angle, average slip, and rupture process (Headquarters for Earthquake Research Promotion, 2017). In this study, the rise time was assumed to be 0 s because the slip was assumed to be instantaneous, and therefore, the source area and initial tsunami were assumed to coincide. For the other parameters, we used the source fault model (Table 1; version 2024/1/15) estimated by the Geospatial Information Authority of Japan based on crustal deformation data obtained from electronic reference points and assuming two rectangular faults (Geospatial Information Authority of Japan, 2024b). The theoretical estimation of land surface deformation based on the fault model proposed by Okada (1985) was used to analyze the initial tsunami water level.

Delft3D, developed by Deltares (2011), was used to analyze tsunami propagation, which can be modeled in two or three dimensions. The two-dimensional (2D) analysis used in this study is equivalent to the nonlinear long-wave equation model commonly used in tsunami and storm surge analysis (Takagi et al., 2020). The alternating direction implicit (ADI) method was used for time integration, and the cyclic method was used for the spatial discretization of advection terms. The flooding method can also be used; however, we selected the cyclic method because land inundation was not considered in this study. A spherical coordinate was used in the present simulations, involving three interconnected regions with the grid spacing of approximately 900–1000 m (Domain 1), 300–333 m (Domain 2), and 100–111 m (Domain 3), as shown in Fig. 1. Bathymetric data from the General Bathymetric Chart of the Oceans (GEBCO) was used for bathymetry. Domains were interconnected using the domain decomposition method, a parallel computing method. This method is suitable for large-scale analysis because it divides the region into small non-overlapping regions, analyzes each region individually, and finds the solution for the entire region through iterative calculations. The time step had to be sufficiently small to ensure a stable analysis even in the narrowest third region; therefore, based on preliminary simulation results, the time step was set to 0.6 s. The total simulation time was limited to 80 min from the origin time of the earthquake due to the reoccurrence of reflected waves at the boundary of Domain 1 beyond this time. For bottom friction, Manning's roughness coefficient, often used in tsunami analysis, was set to 0.025 (s $m^{-1/3}$) (Headquarters for Earthquake Research Promotion, 2017).

In the next section, the coastal conditions are briefly introduced, and the characteristics of tsunami propagation in Toyama Bay and the intensified tsunamis in Iida Bay are explained based on the numerical simulation. The tsunami that caused the damage to the breakwater at Iida Port is also discussed based on wavelet analysis and monitoring camera images.

3. Results and discussion

3.1. Coastal conditions identified in field surveys

Fig. 2 shows tsunami heights based on publicly available runup and inundation measurements (see **Appendix**). The number of observation points in the inner area of Toyama Bay was small because it was difficult to distinguish whether drifting debris was caused by the tsunami or by general high waves. In contrast, numerous observation points were present on the coast of the Noto Peninsula because clear tsunami watermarks remained on the walls of many inundated buildings. Large tsunamis were observed in Iida Bay, located at the tip of the Noto Peninsula, reaching more than 3 m above sea level.

As shown in Fig. 3(1), tree branches and trash were deposited extensively in front of the coastal dike in Namerikawa, Toyama Prefecture; however, definitively attributing these deposits to the tsunami is challenging. On January 1, when the earthquake occurred, Toyama Bay experienced stormy weather. According to the wave observation system called NOWPHAS, a significant wave height of 2.52 m was observed in the Fushiki-Toyama port at 16:20, 10 min after the earthquake. This height was significantly higher than the wave heights of 0.09 m and 0.46 m observed on December 31 and January 2 at the same time, respectively. As shown in Fig. 4, water levels in Toyama Bay were monitored at three tide stations with their names of Toyama (Station 1), Fushiki-Toyama (Station 2), and Nanao (Station 3), where maximum water levels of 0.75 m, 0.83 m, and 0.37 m, respectively, were observed. At stations 1 and 2, the maximum water level was attained 25–27 min after the earthquake. However, the first and second tsunami waves, which were slightly smaller, arrived before the maximum water level. At station 3, located in the inner part of the bay (Nanao Bay), small water surface fluctuations occurred immediately after the earthquake; however, the main tsunami arrived later than at stations 1 and 2, approximately 40 min after the earthquake.

A topographic survey by the Japan Coast Guard immediately after the earthquake revealed a submarine landslide of approximately 500 m long and 80 m wide in Toyama Bay, with depths of up to 40 m. A seafloor slope 30 km offshore of the Noto Peninsula collapsed over a length of 1.6 km (Japan Coast Guard, 2024). Submarine landslides are speculated to have caused an early tsunami before the arrival of the main seismic tsunami (The Japan News, 2024).

At Iida Port, a breakwater section on the north side collapsed (Fig. 3 (3)). The tsunami caused substantial damage: numerous ships sank or were washed up on the wharf and numerous cars were washed away (Fig. 3(4)). The tsunami damage was also evident at Ukai Fishing Port, located 4 km south of Iida Port. Part of the breakwater on the north side of the port collapsed and fishing boats were washed ashore (Fig. 3(5,6)). The breakwaters on the north side of Ukai Fishing Port were damaged rather than the main breakwaters on the east side, suggesting that the

Table 1
Earthquake source fault model proposed by the Geospatial Information Authority of Japan.

Longitude (°)	Latitude (°)	Depth (km)	Length (km)	Width (km)	Strike angle (°)	Dip angle (°)	**Slip angle (°)**	Average slip (m)
136.608	37.185	1.8	63.8	11.9	46.9	26.0	124.4	3.85
137.037	37.439	1.2	76.0	10.8	56.9	59.0	99.3	4.31

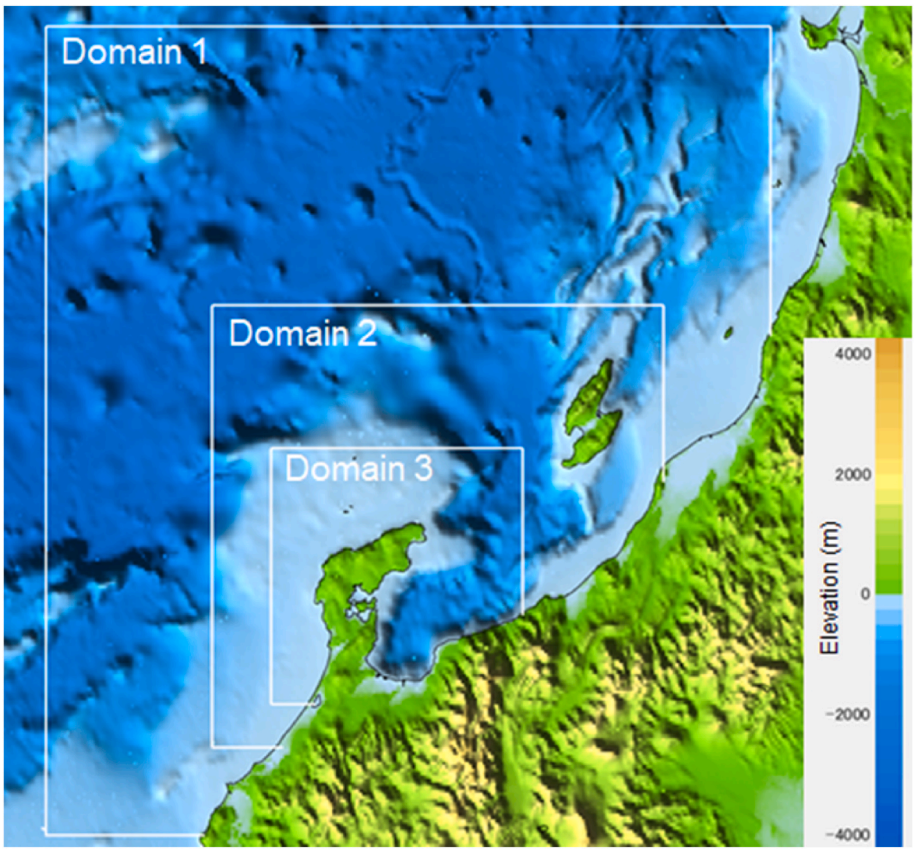

Fig. 1. Tsunami analysis area (computational grid spacing: Domain 1: 0.009° (approximately 900–1000 m), Domain 2: 0.003° (300–333 m), Domain 3: 0.001° (100–111 m)). Domain 3 focuses on the Noto Peninsula, including Toyama Bay and Iida Bay.

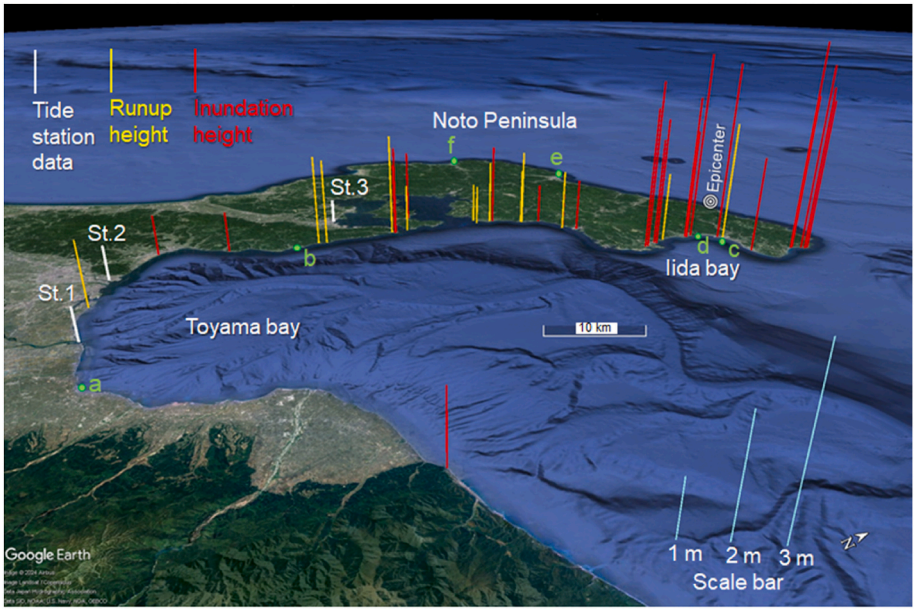

Fig. 2. Tsunami height map created based on observational data (white, yellow, and red bars indicate maximum tsunami heights at tide stations, runup heights, and inundation heights, respectively). Data from tsunami observations conducted by Japan Meteorological Agency, Japan Society of Civil Engineers (Coastal Engineering Committee), and Heidarzadeh et al. (2024) were used in creating the map. Measured data are shown in the table in the Appendix. Points a–f indicate our survey locations.

tsunami originated from a peculiar direction.

Higashihama Fishing Port (Fig. 3(2)) is approximately 50 km south of Iida Bay. The tsunami at this port is less than 2 m high (Fig. 2). Although the earthquake and liquefaction damaged many parts of the port, the tsunami did not appear to have caused notable damage. However, sand and gravel were left on top of the breakwater, suggesting

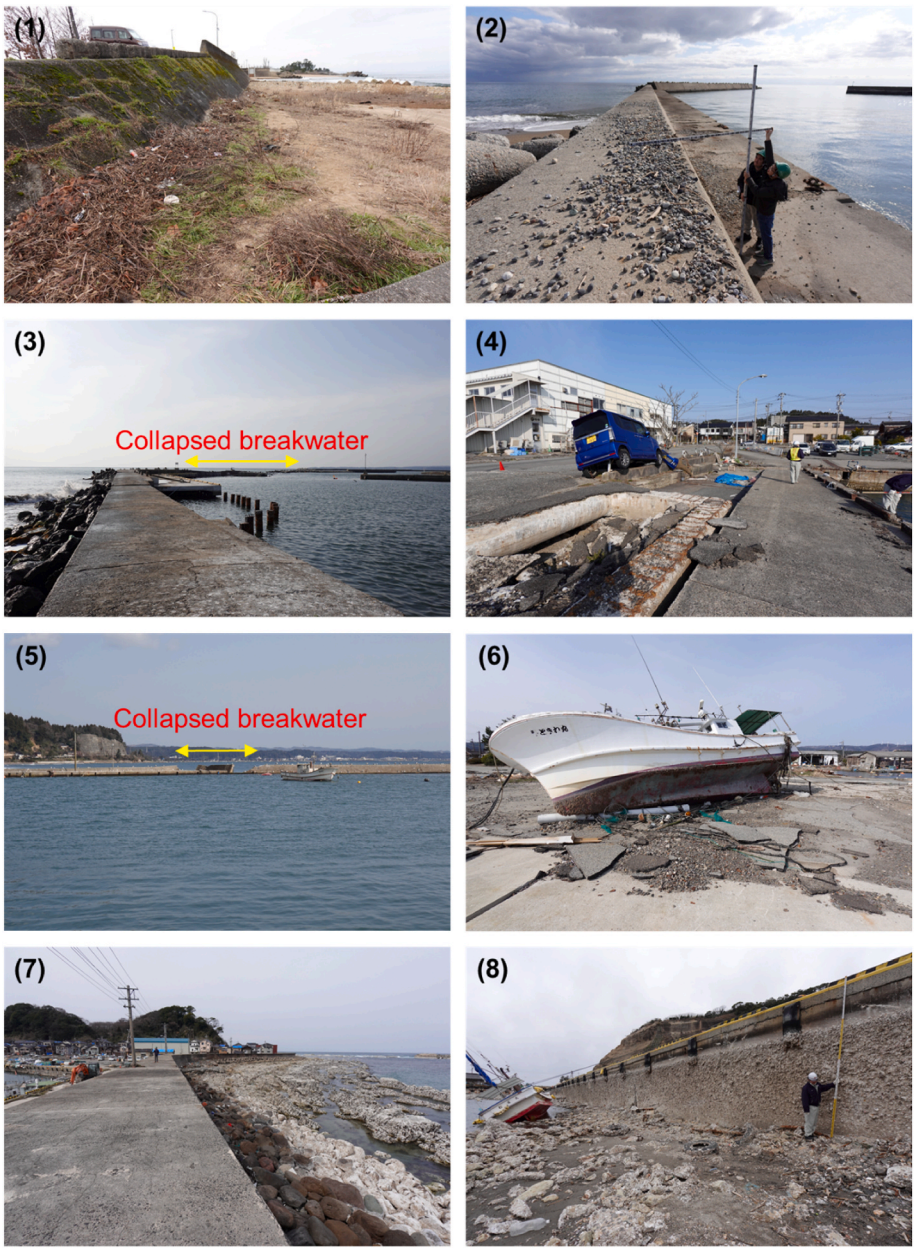

Fig. 3. Photographs acquired during our field surveys after the 2024 Noto Peninsula Earthquake. **(1)** Namerikawa City, Toyama Prefecture. Location: point a in Fig. 2 (137.320°E, 36.758°N), photo taken on 2024/2/2. **(2)** Higashihama Fishing Port, Ishikawa Prefecture. Location: point b in Fig. 2 (137.051°E, 36.978°N), photo taken on 2024/2/2. **(3, 4)** Iida Port, Ishikawa Prefecture. Location: point c in Fig. 2 (137.266°E, 37.436 °N), photo taken on 2024/3/19. **(5, 6)** Ukai Fishing Port, Ishikawa Prefecture. Location: point d in Fig. 2 (137.245°E, 37.402 °N), photo taken on 2024/3/19. **(7)** Wajima Port, Ishikawa Prefecture. Location: point e in Fig. 2 (136.902°E, 37.404°N), photo taken on 2024/3/19. **(8)** Kaiso Fishing Port, Ishikawa Prefecture, where an uplift of nearly 4 m occurred. Location: point f in Fig. 2 (136.728°E, 37.293°N), photo taken on 2024/3/19.

the tsunami overflew the breakwater (3 m above the water surface). Although the tsunami did not cause substantial damage to the port facilities as it did in Iida Bay, it may have affected ships and moorings in the port.

Our survey confirmed that a significant uplift of 1–4 m occurred in Wajima Port (Fig. 3(7)) and Kaiso Fishing Port (Fig. 3(8)). The uplifted seawater is thought to have generated a tsunami; however, no obvious damage from the tsunami was observed at these locations. According to the Chunichi Shimbun newspaper (2024), no major tsunami damage was reported from Kawaura Village, Suzu City at the northern end of the Noto Peninsula to Wajima City, indicating that the sudden uplift may have helped to reduce the impact of the tsunami.

3.2. *Characteristics of tsunami propagation*

The tsunami simulation shown in Fig. 5 indicates that the initial water level generated on the east-west extension of the fault was split into north- and southward moving tsunamis immediately after the earthquake (Fig. 5a), and that most of the energy of the southward moving tsunami was directed into Toyama Bay (Fig. 5b, c, d). The tsunami did not reach the innermost part of Toyama Bay until after 25 min (Fig. 5e), and the water level was not extremely high because the energy was dispersed by that time. The first tsunami hit Iida Bay 20 min later (Fig. 5d). However, a water level rise occurred at 35 min (Fig. 5f), likely caused by the second and subsequent tsunamis.

In the Iida Spur, referring to waters shallower than 300 m spreading

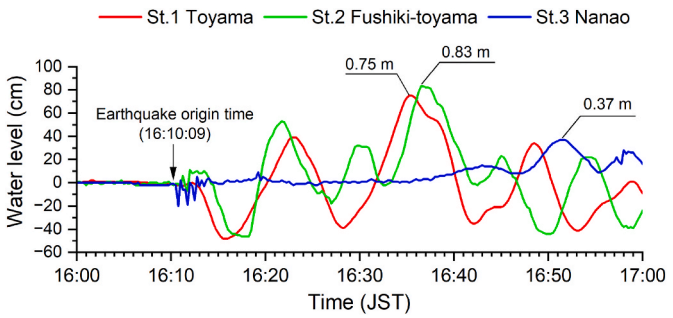

Fig. 4. Water level anomalies from the level at 16:00 at three tide stations. Data are from the Japan Meteorological Agency for site Station 1 and Ministry of Land, Infrastructure, Transport and Tourism for Stations 2 and 3.

out like a tongue off the coast of Iida Bay, slow-moving tsunamis hit Iida Bay while retaining their energy without substantial dissipation. Additionally, wave refraction, inducing energy concentration, occurred due to the steep slope at the boundary between the Toyama Trough, which is more than 900 m deep, and the Iida Spur. Particularly high tsunamis were observed in Iida Bay likely because the tsunami energy converged on the Iida Spur because of this so-called lens effect.

Fig. 6 shows the highest water level distribution determined from numerical simulation results within an hour of the earthquake. It should be noted that most of the energy of the tsunami that propagated toward Toyama Bay surged into Iida Bay. Tsunamis of 2.5 m or higher occurred at three locations: the tip of the Noto Peninsula, the center of Iida Bay, and near the southern cape. These findings are consistent with the distribution of tsunami observations in Fig. 2. Therefore, the tsunami, which advanced from offshore, is inferred to have behaved in a further complicated manner around and within Iida Bay.

3.3. Unique characteristics of tsunamis in Iida Bay

According to the numerical simulation results, the first tsunami wave arrived at the coast of Iida Bay around 20 min after the earthquake. The analytically highest tsunami water level in Iida Bay was 2.5 m. The tsunami height was not uniform within the bay; waves were particularly high in the area from Iida Port to Ukai Fishing Port in the central part of the bay (Fig. 6). This finding is consistent with survey reports stating that the area around Ukai Fishing Port was the most widely flooded in the earthquake (Geological Survey of Japan, 2024b).

A monitoring camera overlooking Iida Bay installed on the roof of Suzu City Hall recorded the tsunami hitting Iida Port (Fig. 7). In this video, the first wave arrives around 20 min after the earthquake, which

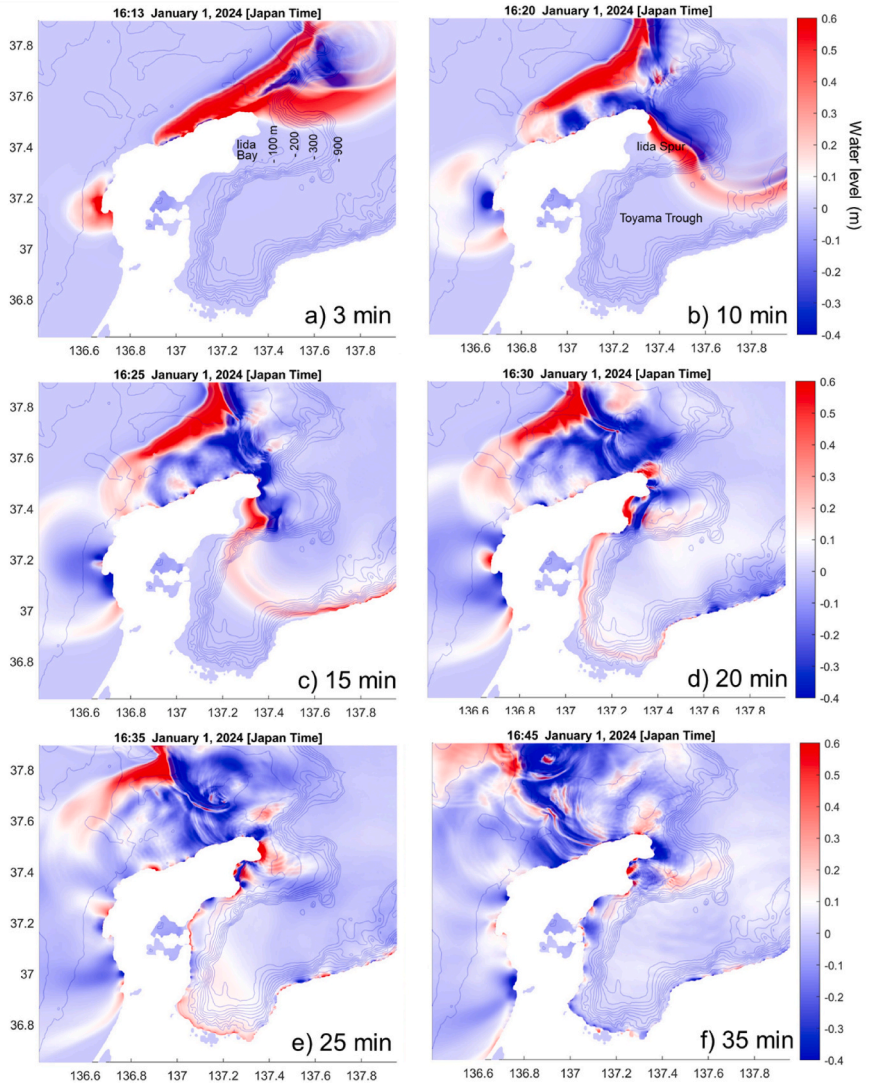

Fig. 5. Tsunami propagation in the numerical simulation (situation from 3 to 35 min after the earthquake). A tongue-shaped shallow water area termed the Iida Spur extends off the northeastern coast of the Noto Peninsula.

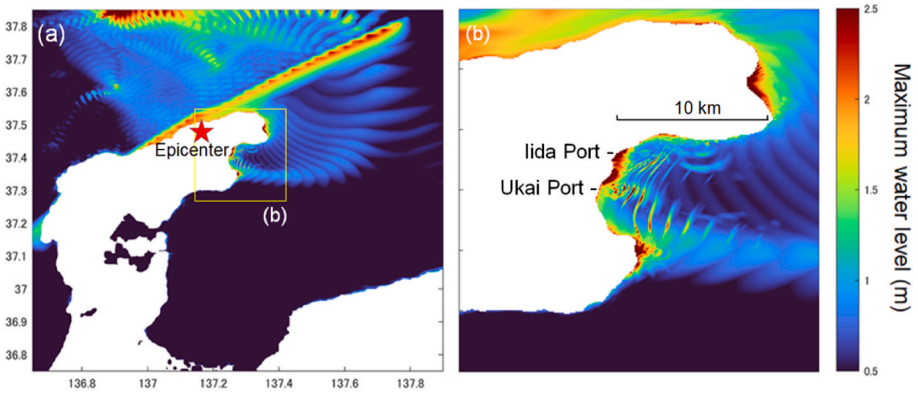

Fig. 6. Simulated maximum water levels around (a) Noto Peninsula and (b) Iida Bay.

is consistent with the numerical calculation results. The waves appear directly from offshore because the wave direction is perpendicular to the coastline. Tsunami overflow appears to occur in the northern section of the breakwater (left side of the photograph in Fig. 7), with the water level rising to near the top of the breakwater at the port entrance. In the video, the water level drops at 25 min; therefore, the oscillatory period

Fig. 7. Images from a monitoring camera overlooking Iida Bay installed on the roof of Suzu City Hall showing the arrivals of the tsunamis at Iida Port (ANN News: https://www.youtube.com/watch?v=T_839fN7ZNU&t=4s).

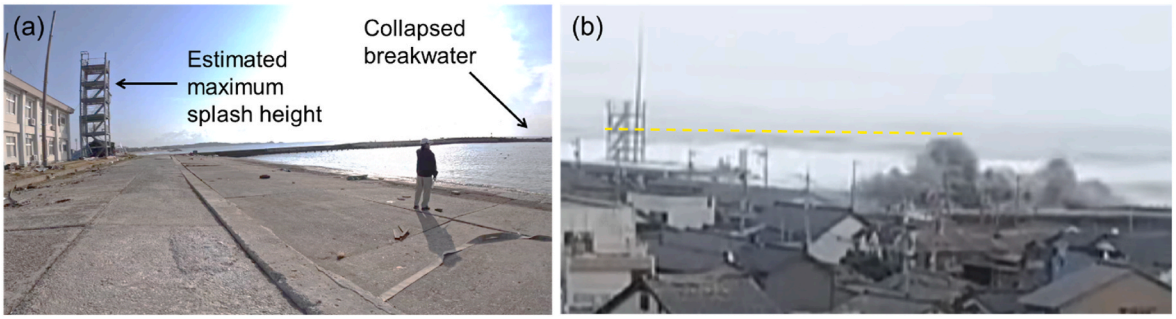

Fig. 8. (a) Tsunami evacuation tower behind Iida Port. According to an evacuation map of Suzu City, the top 5th floor is 14.1 m above sea level. photo taken on 2024/3/19 (b) The tsunami splash possibly reached the same height as the 4th floor of the evacuation tower (ANN News: https://www.youtube.com/watch?v=T_839fN7ZNU&t=4s).

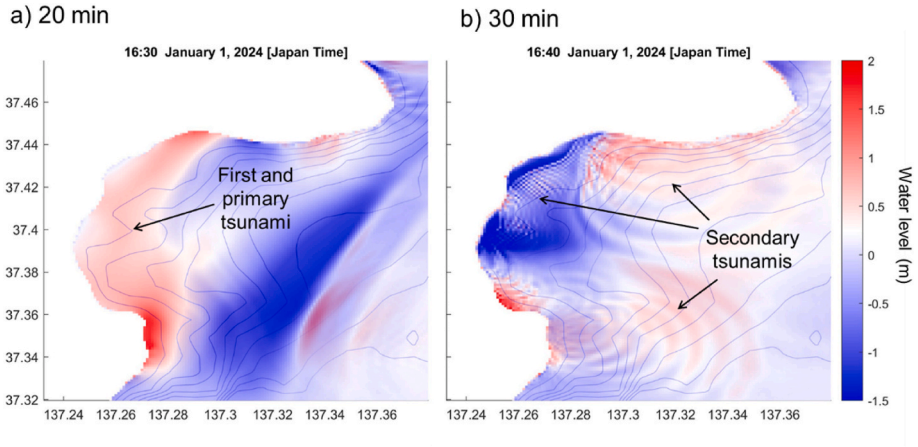

Fig. 9. First to fourth tsunami waves in the numerical simulation results. Bathymetry contour lines are drawn every 10 m.

of the first tsunami wave is estimated to have been less than 10 min.

A clear second wave can be observed around 30 min after the earthquake. In addition to the tsunami advancing from offshore, white waves appear on the north side (left side of the photograph). A bore-like tsunami is moving along the coastline from north to south. At 31 min, the white waves violently hit the north breakwater of Iida Port. Therefore, the impact at this time may have caused to damage the breakwater (Fig. 3(3)). The splash caused by the tsunami collision reached the fourth floor of the evacuation tower behind the port (Fig. 8). As the fifth floor is 14.1 m above sea level, the splash was presumed to reach at least 10 m above sea level.

A detailed numerical analysis of the tsunami propagation situation in Iida Bay revealed that second, third, and fourth waves with shorter periods arrived after the first wave (Fig. 9). The third and fourth waves were diffracted from the north and south capes, these multiple waves possibly intersected near Iida Port, amplifying the tsunami and expanding the damage around the port and the port facility itself.

Fig. 10 shows the results of the continuous wavelet transform using the MATLAB Wavelet Toolbox. It shows how the periodic components of the tsunami changed over time in the output of water level time series data near Iida Port. According to these results, the first wave appeared around 20 min after the earthquake, after which reflection appears to occur. The oscillation period of the primary tsunami energy is estimated to have been 5–10 min, which is consistent with the period inferred from

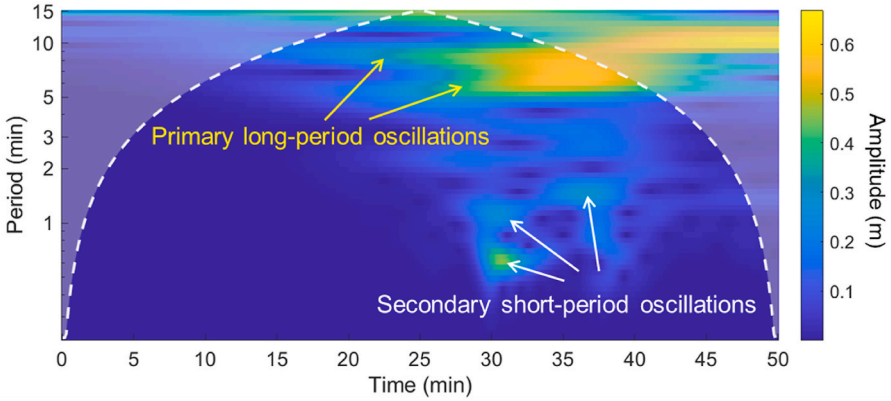

Fig. 10. Wavelet scalogram based on the numerical output of water level time series data near Iida Port.

Fig. 7. In contrast, a short-period tsunami component with less than 2 min can be detected within 30–40 min of the earthquake. These secondary tsunami energies are considered to correspond to the 2nd, 3rd, and 4th waves in Fig. 9. While the tsunami energy from the first wave remained in the bay, the second and subsequent tsunamis overlapped, and this is thought to have caused significant flood damage around Iida Port and Ukai Fishing Port.

4. Conclusions

In the aftermath of the 2024 Noto Peninsula Earthquake on January 1st, 2024, tsunamis arrived at multiple locations; however, a particularly large tsunami occurred in Iida Bay on the Noto Peninsula, causing unprecedented damage to ports and residential areas in Iida Bay. This study clarified the causality between the severe damage and the tsunami propagation characteristics by analyzing information from field surveys, numerical analysis, and monitoring cameras. First, the tsunami energy was significantly concentrated in the Iida Spur, a relatively shallow water that spreads out like a tongue off the coast of Iida Bay. The tsunami energy concentrated off the coast directly proceeded into Iida Bay, without substantial attenuation. Second, after the first tsunami reached the bay, it caused diffraction at the two capes and multiple reflections, generating two or more short-period tsunamis overlapping at specific locations such as Iida Port and the Ukai Fishing Port. Although the estimated tsunami heights in the entire Iida Bay exceeded 3 m above sea level, in Iida Port, the tsunami hit the breakwater, causing a splash of more than 10 m. This study highlights that the damage caused by the tsunamis in Iida Bay was greatly influenced by local conditions, including the topography of the ocean floor, the shape of the coastline, and the location of coastal facilities, in addition to fundamental seismic factors such as the magnitude, size, and location of the earthquake. The findings of the present study suggest that multiple tsunamis may overlap energetically within a bay, requiring further advanced countermeasures to anticipate such localized damage.

CRediT authorship contribution statement

Hiroshi Takagi: Writing – review & editing, Writing – original draft, Visualization, Methodology, Investigation, Funding acquisition, Data curation, Conceptualization. **Nabiel Luthfi Siddiq:** Investigation. **Feldy Tanako:** Investigation. **Daryl Paul Balita De La Rosa:** Investigation.

Declaration of competing interest

There are no conflicts of interest to declare.

Data availability

Data will be made available on request.

Appendix

Table A1
Tsunami height measured by the survey groups of the Japan Meteorological Agency, the Japan Society of Civil Engineers, and Heidarzadeh et al. (2024)

Name of the location	Longitude (°)	Latitude (°)	Height from the sea level (m)	Type	Survey group
Toyama Prefecture, Asahi Town, Miyazaki Fishing Port	137.590308	36.974140	1.4	Inundation	Japan Meteorological Agency
Toyama Prefecture, Imizu City, Kairyuu shin-machi	137.137114	36.771877	1.5	Runup	Japan Meteorological Agency
Ishikawa Prefecture, Suzu City, Iida Port	137.263639	37.434217	4.3	Inundation	Japan Meteorological Agency
Ishikawa Prefecture, Suzu City, Ukai Fishing Port	137.245642	37.401417	2.7	Inundation	Japan Meteorological Agency
Ishikawa Prefecture, Noto Town, Koiji Beach	137.239930	37.370962	1.7	Runup	Japan Meteorological Agency
Ishikawa Prefecture, Noto Town, Matsunami Fishing Port	137.248638	37.356829	3.1	Inundation	Japan Meteorological Agency
Ishikawa Prefecture, Noto Town, Uchiura Sports Park	137.252741	37.342535	4.0	Inundation	Japan Meteorological Agency
Ishikawa Prefecture, Noto Town, Ushitsu Fishing Port	137.150022	37.301147	1.3	Inundation	Japan Meteorological Agency
Ishikawa Prefecture, Nanao City, Unoura Fishing Port	137.053470	37.102246	1.8	Inundation	Japan Meteorological Agency
Ishikawa Prefecture, Nanao City, Sazanami Fishing Port	137.048007	37.012544	2.2	Runup	Japan Meteorological Agency
Ishikawa Prefecture, Noto Town, Matsunami Fishing Port	137.245139	37.355833	2.6	Inundation	Japan Society of Civil Engineers
Ishikawa Prefecture, Noto Town, Nunoura-taku	137.253167	37.338889	3.4	Inundation	Japan Society of Civil Engineers
Ishikawa Prefecture, Noto Town, Fujinami Fishing Port	137.136903	37.288056	1.5	Runup	Japan Society of Civil Engineers
Ishikawa Prefecture, Noto Town, Shichimi Fishing Port	137.090178	37.254167	1.9	Runup	Japan Society of Civil Engineers
Ishikawa Prefecture, Noto Town, Ukawa	137.086925	37.254167	1.4	Runup	Japan Society of Civil Engineers
Ishikawa Prefecture, Anamizu Town, Ukagawa	137.066583	37.220278	1.6	Runup	Japan Society of Civil Engineers
Ishikawa Prefecture, Anamizu Town, Maenami	137.065633	37.203333	1.0	Runup	Japan Society of Civil Engineers
Ishikawa Prefecture, Anamizu Town, Okinami	137.053886	37.203333	1.0	Runup	Japan Society of Civil Engineers
Ishikawa Prefecture, Suzu City, Awazu Beach	137.339746	37.484887	4.9	Inundation	Japan Society of Civil Engineers
Ishikawa Prefecture, Suzu City, Takojima Town	137.324960	37.438876	2.3	Inundation	Japan Society of Civil Engineers
Ishikawa Prefecture, Suzu City, Iida Town	137.268422	37.438583	2.9	Runup	Japan Society of Civil Engineers
Ishikawa Prefecture, Suzu City, Houryu Town	137.243025	37.408649	4.5	Inundation	Japan Society of Civil Engineers
Ishikawa Prefecture, Suzu City, Houryu Town	137.242455	37.401066	3.5	Inundation	Japan Society of Civil Engineers
Ishikawa Prefecture, Nanao City, Notojima, Kouda Town	137.000000	37.135556	1.8	Inundation	Japan Society of Civil Engineers
Ishikawa Prefecture, Nanao City, Notojima, Nozaki Town	137.050536	37.118611	1.2	Runup	Japan Society of Civil Engineers
Ishikawa Prefecture, Nanao City, Unoura Town	137.049176	37.100020	2.5	Runup	Japan Society of Civil Engineers
Ishikawa Prefecture, Nanao City, Iori Town	137.050559	37.021440	2.1	Runup	Japan Society of Civil Engineers
Ishikawa Prefecture, Nanao City, Sazanami Town	137.268422	37.438583	2.4	Runup	Japan Society of Civil Engineers
Toyama Prefecture, Himi City, Kubo	136.996800	36.845600	1	Inundation	Heidarzadeh et al. (2024)
Toyama Prefecture, Himi City, Kosakai	137.026000	36.917000	1	Inundation	Heidarzadeh et al. (2024)
Ishikawa Prefecture, Suzu City, Misaki Town	137.349700	37.501500	3.6	Inundation	Heidarzadeh et al. (2024)
Ishikawa Prefecture, Suzu City, Misaki Town	137.348400	37.499300	3.7	Inundation	Heidarzadeh et al. (2024)
Ishikawa Prefecture, Suzu City, Misaki Town	137.349400	37.497800	3.7	Inundation	Heidarzadeh et al. (2024)
Ishikawa Prefecture, Suzu City, Misaki Town	137.349400	37.497800	3.9	Inundation	Heidarzadeh et al. (2024)
Ishikawa Prefecture, Suzu City, Misaki Town	137.346400	37.495000	4.4	Inundation	Heidarzadeh et al. (2024)
Ishikawa Prefecture, Suzu City, Misaki Town	137.339700	37.486900	3.7	Inundation	Heidarzadeh et al. (2024)

(*continued on next page*)

Table A1 (*continued*)

Name of the location	Longitude (°)	Latitude (°)	Height from the sea level (m)	Type	Survey group
Ishikawa Prefecture, Nanao City, Unoura Fishing Port	137.052100	37.103800	2.2	Inundation	Heidarzadeh et al. (2024)
Ishikawa Prefecture, Anamizu Town, Ukagawa	137.066700	37.224000	2	Inundation	Heidarzadeh et al. (2024)
Ishikawa Prefecture, Noto Town, Nagashima Island	137.130600	37.291700	1	Inundation	Heidarzadeh et al. (2024)
Ishikawa Prefecture, Noto Town, Yanami Fishing Port	137.097600	37.273600	1	Inundation	Heidarzadeh et al. (2024)

References

Chunichi Shimbun newspaper, 2024. https://www.chunichi.co.jp/article/834017 (in Japanese).

Deltares, 2011. Delft3D-FLOW – Simulation of Multi-Dimensional Hydrodynamic Flows and Transport Phenomena, Including Sediments, vol. 690p. User Manual Delft3D-FLOW.

Geological Survey of Japan, 2024a. https://www.gsj.jp/hazards/earthquake/noto2024/noto2024-04.html (in Japanese).

Geological Survey of Japan, 2024b. https://www.gsj.jp/hazards/earthquake/noto2024/noto2024-06.html (in Japanese).

Geospatial Information Authority of Japan, 2024a. https://www.gsi.go.jp/uchusokuchi/20240101noto_insar.html (in Japanese).

Geospatial Information Authority of Japan, 2024b. https://www.gsi.go.jp/common/000254306.pdf (in Japanese).

Hatori, T., 1990. Magnitudes of the 1833 yamagata-oki earthquake in the Japan sea and its tsunami. Zisin 43, 227–232 (in Japanese).

Headquarters for Earthquake Research Promotion, 2017. Tsunami Prediction Method for Earthquakes with Characterized Source Faults (Tsunami Recipe), 38 pages (in Japanese).

Heidarzadeh, M., Ishibe, T., Gusman, A.R., Miyazaki, H., 2024. Field surveys of tsunami runup and damage following the January 2024 Mw 7.5 Noto (Japan Sea) tsunamigenic earthquake. Ocean Eng.

Japan Coast Guard, 2024. https://www.kaiho.mlit.go.jp/info/kouhou/r6/k240222/k240222.pdf (in Japanese).

Japan Meteorological Agency, 2024. https://www.jma.go.jp/jma/press/2401/26a/20240126_tsunamichousakekka.pdf (in Japanese).

NHK, 2024. Article dated February 20. https://www3.nhk.or.jp/news/html/20240220/k10014364401000.html (in Japanese).

Okada, Y., 1985. Surface deformation due to shear and tensile faults in a half-space. Bull. Seismol. Soc. Am. 75, 1135–1154.

Takagi, H., Tomiyasu, R., Oyake, T., Araki, T., Mori, K., Matsubara, Y., Ninomiya, Y., Takata, Y., 2020. Tsunami intrusion through port breakwaters enclosed with self-elevating seawalls. Ocean Eng. 199, 13p.

The Japan News, 2024. https://japannews.yomiuri.co.jp/society/noto-peninsula-earthquake/20240105-160060/ (in Japanese).

Yuhi, M., Abe, N., 2013. Numerical simulation of historical tsunamis around Noto Peninsula, Ishikawa, Japan. J. Jpn. Soc. Civ. Eng. 69 (2), 491–496 (in Japanese).

Nikkei XTECH, 2024. https://xtech.nikkei.com/atcl/nxt/column/18/02706/010900026/ (in Japanese).